Shuttle Navigation System for Entry and Landing Mission Phases

Bernard A. Kriegsman* and Yee-Chee Tao†
Charles Stark Draper Laboratory, Cambridge, Mass.

An on-board filter is designed to efficiently process inertial-measurement-unit data in combination with data from other external navaids such as TACAN, one-way Doppler, baro-altimeter, radar altimeter, and MLS. During the approach phase (altitude above 12,000 ft) a 13-state minimum-variance filter is recommended, with position (3), velocity (3), IMU alignment (3), and various navaid correlated errors (4) as state elements. The navaid errors are modeled as first-order Markov processes, with state (process) noise employed in the extrapolation procedure to account for unmodeled errors. A simple underweighting technique is employed to insure good navigation-system performance in the presence of large initial-condition errors. During the terminal phase (altitude below 12,000 ft) a 6-state filter is used, including as state elements only position (3) and velocity (3). Prestored weighting vectors are used here, based on the last computed values for the preceding approach phase.

Introduction

THE task of safely landing the unpowered shuttle orbiter vehicle on a selected runway poses new and difficult navigation-system design problems. Large navigation errors can build up during the period of entry blackout (e.g., 5-10 nmi and 30-50 fps) when the on-board inertial measurement unit (IMU) is the sole available navaid. Area navaid information from sensors such as TACAN or one-way Doppler (OWD) must be processed as soon as possible after blackout, so that trajectory deviations can be determined and corrected when the vehicle still has sufficient energy. The final approach must utilize high-accuracy information from navaids such as the Microwave Landing System (MLS) to satisfy touchdown rms error requirements dictated by runway width and landing gear structure (e.g., about 4 ft altitude and cross-track position, and 0.2 fps for vertical velocity).

Many different types and combinations of navaids have been studied for possible use during the shuttle entry and landing mission phases. Early studies used VOR/DME information in combination with baro-altimeter data in the post-blackout period.[1,2] Ground-based precision ranging devices were also seriously considered at this time for use both after blackout and in the vicinity of the touchdown point.[3,4] More recent studies have been concerned with conventional ILS systems[5] and proposed MLS systems[6,7] as terminal area navaids. In addition, OWD has been extensively investigated as a potential area or terminal-phase navaid.[8]

This paper describes studies performed at CSDL (Charles Stark Draper Laboratory, Cambridge, Mass.) to assist RI (Rockwell International Inc., Downey, Calif.) and NASA/JSC in the development of a baseline navigation system for the shuttle. A single TACAN station is assumed as the area navaid in combination with a baro-altimeter. OWD is considered as an alternate choice or backup system to TACAN. In the terminal area the prime navaid is an MLS configuration, supplemented by radar altimeter data close into the touchdown point.

Presented as Paper 74-866 at the AIAA Mechanics and Control of Flight Conference, Anaheim, California, August 5-9, 1974; submitted August 26, 1974; revision received November 14, 1974.The authors express their appreciation to R. Savely of NASA/JSC, F. Marcus of CSDL, and E. Muller of CSDL for helpful suggestions and discussions during the course of study.

Index category: Spacecraft Navigation, Guidance, and Flight-Path Control Systems.

*Section Chief, Guidance and Navigation. Member AIAA.

†Draper Fellow.

Certain aspects of the overall problem have a strong influence on the navigation-system design. In particular these are: 1) The need for small computation-cycle times during the terminal phase to avoid overloading the on-board computer's processing capability. 2) The presence of significant time-correlated errors in the IMU and other navaids. 3) The desirability of proper navigation-filter operation (convergence) with large initial-condition errors (e.g. 3-sigma position and velocity errors). 4) The extremely difficult touchdown accuracy requirements.

For convenience, the problem is considered here in two separate modes: an approach phase starting at an altitude of 130,000 ft and extending down to about 12,000 ft, and a terminal phase continuing thereafter to touchdown. As will be seen, different navigation filters are utilized in these phases to best meet the problem requirements.

Basic Assumptions

Trajectory Characteristics

The prime interest in this paper is on the period of flight starting when the vehicle is at an altitude of about 130,000 ft (end of blackout) and terminating when the landing gear first touches the runway. At the starting point the vehicle is about 120 nmi from the runway and travelling towards it with a velocity of about 6000 fps. The unpowered vehicle decelerates fairly rapidly at first, and then more slowly, until it finally arrives at the touchdown point with a relative velocity of about 500 fps.

The assumed trajectory profile is shown in Figs. 1 and 2. As the vehicle approaches the landing area, a 180° turn is made to dissipate excess energy. The final approach (below 12,000 ft) is made at a relatively steep flight-path angle (about 19° down from the local horizontal plane) with an essentially straight-in ground track. At an altitude of about 1000 ft a pull-up maneuver is initiated to reduce the vertical component of vehicle velocity to an acceptable touchdown value (about 5-10 fps.

Sensor Modeling

The types of navigation sensors used during the entry and landing phases are shown in Table 1 along with their regions of operation. The IMU is used throughout the trajectory as a prime navaid, providing data at discrete times (e.g., every 0.5-2 sec) on the change in velocity caused by nongravitational forces on the vehicle. In addition, IMU-derived drag is used to

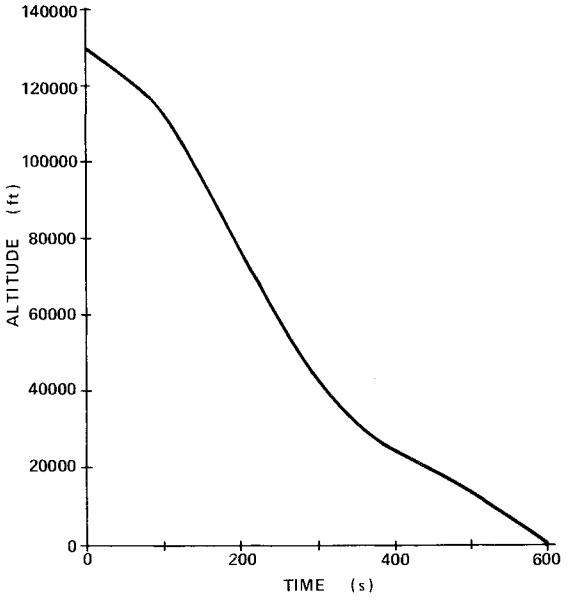

Fig. 1 Reference trajectory altitude profile.

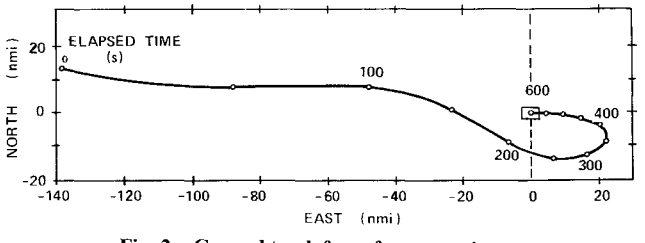

Fig. 2 Ground track for reference trajectory.

Table 1 Navigation measurements utilized

Vehicle Alt (ft)	IMU	TACAN		MLS	Drag Alt	Baro Alt	Radar Alt	OWD
		Range	Az					
130,000	↕	↕	↕		↕			↕
100,000	↕	↕	↕			↕		↕
85,000	↕	↕						↕
69,000	↕	↕	↕					↕
52,000	↕	↕	↕					↕
41,000	↕	↕	↕			↕		↕
20,000	↕	↕	↕	↕		↕		↕
100	↕			↕			↕	
0	↕			↕			↕	

estimate vehicle altitude during the initial flight period above 100,000 ft.[9] TACAN or OWD are used to provide navigation-system updates down to the point of MLS acquisition (about an altitude of 20,000 ft and range of 15 nmi). TACAN provides data on vehicle range and azimuth relative to the ground station, whereas OWD measures the change in range from the vehicle to the ground-based transmitter. The MLS is assumed to include three separate radars which provide extremely accurate measurements of range, elevation angle, and azimuth angle of the vehicle relative to the sensor.

The detailed IMU error model is summarized in Table 2. It is a fairly simple model, based on an inertially-fixed gimballed unit. Three error sources are considered: stable-member alignment, accelerometer bias, and accelerometer scale-factor uncertainty. Over the period of interest these errors are treated as time-invariant bias errors, normally distributed about a zero-mean value. The large alignment errors reflect an extended period of IMU drift (e.g., 1-2 hr) earlier in the flight.

The OWD study model is derived largely from the work of Ref. 8. The basic measurement is a count of Doppler cycles over a short time interval (e.g., 0.5-2 sec). At the assumed transmitter frequency of 2.2×10^9 cps each cycle corresponds to about 0.5 ft of range change. The detailed error model assumed for OWD is given in Table 3. Frequency multiplication is assumed at the receiver to provide the low quantization errors. An order-of-magnitude better performance is assumed for the ground-based frequency standards than for those of the airborne receiver.

The error models for the IMU-derived drag, TACAN, MLS, baro-altimeter, and radar-altimeter measurements are summarized in Table 4. The drag error model is predicated on the technique of Ref. 9, which uses IMU data in combination with a priori models of the density of the atmosphere and the aerodynamic coefficients of the vehicle to infer altitude. The error values reflect modeling errors in density and vehicle aerodynamic data. The TACAN model is based on data from Refs. 10 and 11. The maximum line-of-sight elevation angle for which TACAN azimuth data are processed is 45°.

The baro-altimeter model is based on the information in Ref. 12, which includes errors from uncertainties in the at-

Table 2 IMU error model

Error Source		RMS Value
Stable-member alignment	(mr/axis)	1
Accelerometer bias	(ft/s^2)	0.0017
Accelerom. scale factor	(ppm)	100

Table 3 One-way-Doppler error model

Error Source	RMS Value	Correlation Time
Quantization	0.12 cyc	—
Rec. clock bias	2.0 cps	600 s
Rec. clock random	0.2 cps	—
Trans. clock bias	0.2 cps	∞
Trans. clock random	0.02 cps	—

Table 4 Navaid error models

Measurement Type	RMS Error		Correlation Times (s)
	Random	Correlated	
TACAN range	90 ft	275 ft	400
TACAN azimuth	6 mr	6 mr	400
Drag	5% drag	15% drag	100
Baro altitude	0.03% alt	3% alt	200
MLS range	24 ft	35 ft	∞
MLS elevation	0.2 mr	0.4 mr	∞
MLS azimuth	0.2 mr	0.4 mr	∞
Radar altitude	0.1 ft[a]	1 ft[a]	∞
	20 ft[b]	20 ft[b]	8

[a] Terrain variations off runway.

[b] Sensor errors over runway.

mosphere model, static defect of the pressure port, and instrument noise. A percent-of-altitude type model is used to approximate these effects over the 20,000 to 100,000 ft altitude range of operation. No baro data are processed at vehicle speeds between Mach 0.95 and 1.05.

The MLS model is based on information for an AIL AN/TRN-28A microwave scanning beam landing system given in Ref. 11. A conservative acquisition range of about 15 nmi was assumed, which occurred at an altitude of 20,000 ft on the reference trajectory. The range and azimuth-angle radars were assumed to be colocated along the runway center line 10,000 ft down-range beyond the touchdown point. The elevation radar was placed 200 ft to the side of the touchdown point.

For the radar altimeter two separate models are required, as indicated in Table 4. When the vehicle is over the level runway, extremely high accuracy can be expected. Off the runway, on the other hand, the performance will degrade due to local terrain altitude variations.

Basic Design Philosophy for Overall System

The approach adopted was to utilize IMU data throughout the entry and landing phases as in a conventional fixed-reference frame inertial-navigation system.[13,14] Vehicle position (**r**)‡ and velocity (**v**) are obtained by numerical integration of the equations:

$$\dot{v}=s+g \tag{1}$$

$$\dot{r}=v \tag{2}$$

where **s** and **g** represent, respectively, the nongravitational and gravitational forces per unit mass acting on the vehicle. The nongravitational specific force (**s**) is derived from IMU data, whereas the gravitational specific force (**g**) is computed from estimated vehicle position (**r**).

At discrete time points (e.g., every 2 sec) IMU-derived position and velocity estimates (**r**,**v**) are updated with external navaid information as it becomes available. For mechanization simplicity the navaid measurements are processed sequentially as scalar quantities. At the same time that **r** and **v** are updated, the estimates of certain important time-correlated errors (γ) present in the IMU and external navaids are also updated.

The updating process is based on the weighted difference between the measurement being processed ($\tilde{q}$) and its a priori estimate (q'). The updating equation is most conveniently written as:

$$\hat{x}=x'+w(\tilde{q}-q') \tag{3}$$

where for convenience the quantities being estimated (**r**,**v** and γ) are considered as elements of a higher-order state vector (**x**). The weighting vector used in the processing of the measurement is denoted by **w**.

The computation of the weighting vector (**w**) is a key navigation-system design problem. Two different techniques are used to accomplish this. During the approach phase (altitude greater than 12,000 ft) when computation-cycle time is not critical, a Kalman-type minimum-variance estimator is used. Detailed discussions of the theoretical background of this type of estimator and its application to navigation problems are well documented in the literature.[15-17] During the terminal phase, on the other hand, where computation-cycle time is more critical, simple prestored weighting functions are used.

‡Lower case letters and Greek symbols will generally be reserved for vectors and scalars. Vectors will be indicated by boldface. Upper case letters are reserved for matrices. Differentiation with respect to time is indicated by a dot over the quantity of interest.

Approach-Phase Filter Design

Weighting-Vector Computations

The weighting vectors used here are for a minimum-variance estimator in a full covariance matrix formulation. Basically three quantities are required in the computation of **w**: the covariance matrix of the errors in the estimate of the measurement being processed ($\overline{\alpha^2}$), and the first-order sensitivity of the measurement to changes in the state (**b** or $\partial q/\partial \mathbf{x}$). Using these quantities, the weighting vector is given by:

$$w=\frac{Eb}{b^TEb+\overline{\alpha^2}+\beta} \tag{4}$$

where the term β is used to underweight the navaid measurements. As will be seen, underweighting can greatly improve the filter's performance in the presence of large initial errors.

In order to obtain meaningful values for w, it is necessary to update E after each new measurement has been processed, and extrapolate it between update times. The relation used to accomplish the updating is:

$$E=(I-wb^T)E' \tag{5}$$

where I is an identity matrix, and E' is the a priori value of E. Extrapolation of E between measurements is done by:

$$E_{n+1}=\phi E_n\phi^T+Q \tag{6}$$

where ϕ is the state transition matrix. The matrix Q represents process noise included in the covariance-matrix extrapolation process to compensate for sensor and other errors not directly modeled in the state.

Alternate mechanizations for the minimum-variance estimator have been developed, using the square-root of the covariance matrix (W) rather than the full covariance matrix (E), as described in Refs. 18 and 19. If the on-board computer has sufficient word length, however, the full-covariance formulation is more attractive because of the simpler way in which process noise can be included.

State-Vector Size and Structure

Significant time-correlated errors are assumed to be present in the various sensor measurement data of interest here, as can be seen from Tables 2-4. To most effectively process navaid data, these errors must either be modeled directly in the filter as state elements, or accounted for indirectly by process noise. If the correlated errors are included as state elements, their effect can generally be modeled more accurately, and better navigation-system performance should be obtained. The resultant filter will, however, be more complex and may be more sensitive to modeling errors. If, on the other hand, process noise is used, the error modeling will tend to be less accurate, but a simpler filter is obtained. Acceptable performance can often be obtained, however, with small state-size filters by proper choice of state elements and process noise.

To do a reasonably accurate job of modeling all important navigation-sensor errors, it was found that 16 filter states are required: vehicle position (3), vehicle velocity (3), IMU alighnment errors (3), IMU acceleration measurement errors (3), and various time-correlated navaid errors (4). The basic elements in the state vector and their arrangement is shown in Table 5. All IMU and external navaid time-correlated errors are modeled as first-order Markov processes rather than as constant bias errors because of the greater modeling flexibility that is obtained.

It should be noted that 9 time-correlated measurement errors are modeled, using only 4 state-vector elements since: 1) TACAN and OWD are not used after MLS acquisition; and

Table 5 State-vector arrangement in filter

Vehicle Pos & Vel		IMU Errors		Navaid Time-Correlated Errors			
		Alignment	Accel				
(3)	(3)	(3)	(3)	γ_{TACR}	γ_{TACAZ}	γ_{RECBI}[a]	γ_{DRAG}
$\underline{r}$	$\underline{v}$	$\underline{\gamma}_{AL}$	$\underline{\gamma}_{ACC}$	γ_{MLSR}	γ_{MLSAZ}	γ_{MLSEL}	γ_{BARO}
							γ_{RADH}

[a] OWD receiver clock error

Table 6 Root-mean-square errors at end of blackout

Error Type	Vertical	Cross Track	Down Range
Position (ft)	3750	14,000	15,600
Velocity (ft/s)	4.9	22.0	15.7

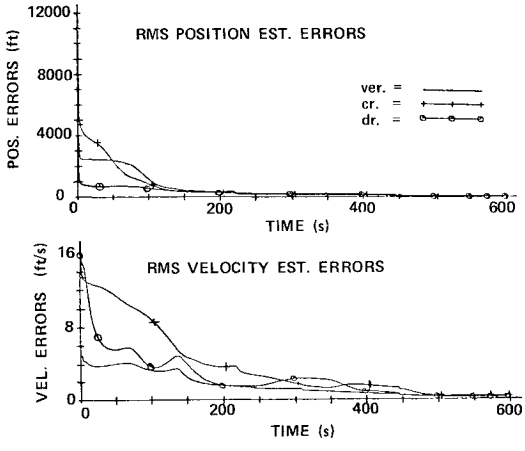

Fig. 3 Root-mean-square errors for 16-state filter (TACAN/MLS).

2) drag, baro-altimeter, and radar-altimeter measurements are not used during the same time periods. When the error type assigned to a given state element is changed, the corresponding row and column of the filter covariance matrix must be reinitialized.

To investigate the effect of state-vector size on navigation-filter performance, series of simulation runs were made for various filter state-vector sizes, ranging from a minimum of 6 elements (position and velocity) to a maximum of 16, as in Table 5. A TACAN station near the runway was assumed as the area navaid. The trajectory characteristics were as given in Figs. 1 and 2, and the sensor models were as in Tables 2-4. Postblackout rms errors were assumed to be about 4 nmi in position and 27 fps in velocity, as indicated in Table 6.

Navigation-system performance data for the two extreme cases, i.e., the 6 and 16 state-vector filters, are shown in Figs. 3 and 4 and Table 7. The rms errors were computed by linear statistical-analysis techniques. In comparing the simulation results, it is seen that there is a significant degradation in navigation accuracy during the first few minutes after blackout when the 6-state filter is used, because of the poorer quality in modeling. In addition, improper correlations developed in the 6-state filter are seen to cause excessibly large velocity errors during the early processing of MLS data.

The studies also indicated no significant degradation in navigation accuracy when either the IMU alignment or IMU acceleration state were omitted from the filter, i.e., the 13-state filter performed about as well as the 16-state one. Going to a 10-state filter by omitting TACAN and MLS time-

Table 7 Effect of state size on post-blackout errors (TACAN as area navaid)

Filter State Size	Time after Blackout (min)	RMS Pos Est Err (ft)			RMS Vel Est Err (ft/s)		
		Vert	Cross Track	Down Range	Vert	Cross Track	Down Range
16 states	1	2260	1790	706	4.2	10.9	5.8
	2	610	540	405	3.3	7.2	4.2
	3	310	310	260	1.7	4.0	2.0
6 states	1	3390	3070	1170	6.3	11.2	8.2
	2	3402	1450	1730	6.3	14.4	14.1
	3	1700	1240	1210	6.7	16.9	7.7

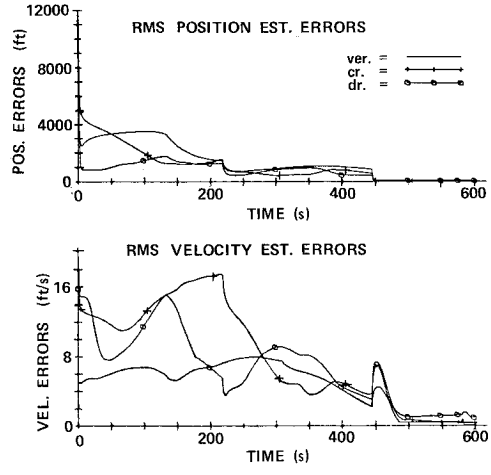

Fig. 4 Root-mean-square errors for 6-state filter (TACAN/MLS).

correlated errors from the filter, on the other hand, did noticeably degrade navigation-system performance.

The conclusion from the simulation runs was that to get best performance in the non-time-critical approach phase, a 13-state filter should be used. The choice between IMU alignment or IMU acceleration errors as filter states was not clear cut, but a slight preference is for IMU alignment at the present time.

Measurement Underweighting

At the end of blackout (altitude of 130,000 ft) position errors may be as large as 12 nmi, and velocity errors as large as 80 fps (3-sigma values). Under these conditions the linear minimum-variance filter may not operate properly during the processing of early measurement data, or in extreme cases the actual navigation errors may not converge to the filter predicted values. This type of behavior is most visible when highly accurate OWD or range measurements are used. The problem is that with large initial errors and highly accurate navaid data, the linear relations used in Eqs. (4-6) do not properly describe the true physical situation. The result is that the filter's estimate of its errors becomes much too optimistic.

Several different techniques have been considered for circumventing this type of problem (e.g., Refs. 15, 16, 20, and 21). The primary interest here, however, is on the following two techniques suggested by Lear[12]: 1) increasing the variance of the error in the a priori estimate of the measurement to be processed; and 2) utilizing a modified Gaussian second-order filter to correct for measurement nonlinearities.§

The first technique is extremely simple. A correction term β is computed from the relation:

$$\beta = k_1 \boldsymbol{b}^T \boldsymbol{E} \boldsymbol{b} \tag{7}$$

§This technique has been very successful in certain orbit-navigation problems.

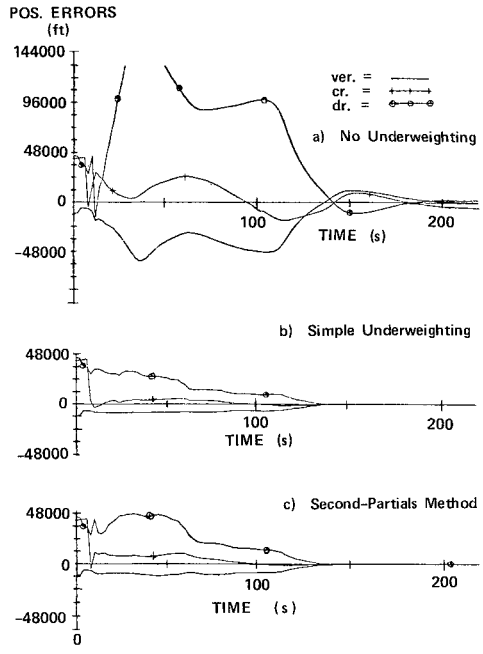

Fig. 5 Effect of underweighting on position errors (OWD/MLS system, 3-sigma initial errors).

This term is then used in the weighting-vector computation [as indicated in Eq. (4)] to reduce **w**. Typically k_1 has been set to 0.2.

The second technique is much more complex. The basic assumptions and theoretical development of the method are given in Ref. 12. A correction term β is computed from the relation:

$$\beta = \frac{1}{4}(\text{trace}\,[H])^2 + \frac{1}{2}\,\text{trace}\,[H^2] \qquad (8)$$

The 6×6 matrix H is given by the relation:

$$H = B\,E_{RV} \qquad (9)$$

where B is a 6×6 matrix of the second partials for the measurement of interest, taken with respect to variations in position and velocity, and E_{RV} is the position-velocity submatrix of the filter's covariance matrix E.

Extensive simulation runs have been made to study both schemes, with up to 10-sigma initial-condition errors in the estimates of both position and velocity. The detailed numerical results are given in Refs. 22 and 23. Some typical test-case results are shown in Fig. 5 for a 3-sigma set of initial-conditions errors with OWD as the area navaid.

As can be seen, both underweighting techniques significantly improve navigation-system performance. Of particular interest is the fact that the simple scheme using $k_1\mathbf{b}^T E\mathbf{b}$ appears to work at least as well as (if not slightly better than) the more complex second-partials method. Numerous test-case runs in Refs. 22 and 23 using other initial-condition error combinations show the same general performance trends.

The study results clearly indicate a much greater need for underweighting with OWD as a navaid than with TACAN. This can be seen from the data of Table 8 where the correction terms (β) computed by the second-partials method are presented for a given test-case run: a) with TACAN as the area navaid; and b) with OWD used instead. For convenience in making comparisons, the data are normalized with respect to the random-error variance for the measurement of interest (α^2).

When test-case initial-condition errors at the 10-sigma level were assumed with an OWD navaid, the performance obtained with either underweighting scheme was unsatisfactory. When the same test-case runs were repeated with TACAN, on the other hand, the performance was much better, as shown in Fig. 6.

Table 8 Correction term for second-partials scheme

Number of Measurement	Correction Term β/α^2		
	OWD	TACAN Range	TACAN Azimuth
1	162	7.3	—
2	50	1.8	—
3	22	0.1	—
4	22	0.08	—
10	9	—	—
20	5	—	—
50	0.05	—	—

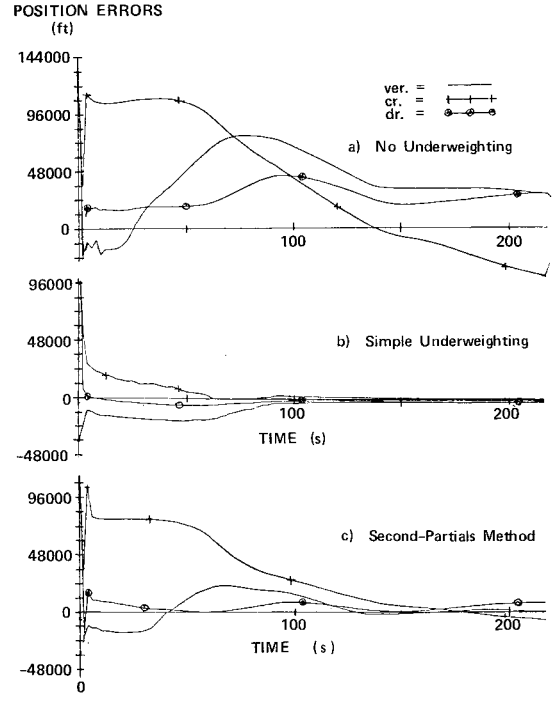

Fig. 6 Effect of underweighting on position errors (TACAN/MLS system, 10-sigma initial errors).

An alternate scheme that has been examined more recently computes a correction β from the relation:

$$\beta = k_2(\delta q)^2 \qquad (10)$$

where the quantity δq represents the actual measurement residual $\bar{q} - q'$. This correction term is employed when the magnitude of δq is greater than 2 or 3 times the filter's predicted rms value $[\,(\mathbf{b}^T E\mathbf{b} + \overline{\alpha^2}\,)\,]^{1/2}$. An appealing feature of this technique is that β is based on actual test-case residuals rather than filter-predicted rms errors. Sufficient analysis has not been made of this scheme at present for proper evaluation. On the basis of the results to date, the recommended underweighting scheme is the simple one which uses $k_1\mathbf{b}^T E\mathbf{b}$.

Terminal-Phase Filter Design

During the terminal phase (altitude below 12,000 ft), the navigation problem is different from that of the preceding approach phase in three different ways: 1) Short computation-cycle times (and high update rates) are of prime importance in this phase. 2) The navigation problem for the most part is in a quasi-stationary mode; i.e., the relevant trajectory characteristics and desired sensor weighting functions do not change

Table 9 Root-mean-square touchdown error requirements

Error Type	Vertical	Cross Track	Down Range
Position (ft)	3	5	80
Velocity (ft/s)	0.2	2	3

Table 10 Root-mean-square navigation error during terminal phase

Filter Description	Altitude (ft)	Pos Est Err (ft)			Vel Est Err (ft/s)		
		V	CT	DR	V	CT	DR
16-state minimum variance	0,000	16	16	33	0.23	0.29	0.25
	2,400	8	7	30	0.22	0.20	0.17
	600	3	5	14	0.23	0.19	0.16
	0	1	4	10	0.07	0.19	0.16
6-state stored weighting functions	0,000	16	16	33	0.23	0.29	0.25
	2,400	9	7	34	0.23	0.23	0.22
	600	7	5	35	0.25	0.24	0.22
	0	1	4	35	0.08	0.22	0.24

rapidly. 3) The touchdown accuracy requirements are very stringent; e.g., rms altitude and cross-track position errors of about 4 ft and vertical velocity errors of 0.2 fps, as shown in Table 9.

Early simulation results using a 16-state filter for both the terminal and approach phases indicated that the vehicle's position errors during the terminal phase were primarily determined by the MLS bias errors. Furthermore, the navigation filter was not able to successfully estimate the MLS angle bias errors during this phase or significantly improve on its previous estimates of IMU time-correlated errors.

Under these conditions it was decided to consider a 6-state filter for the terminal phase (position and velocity only), using prestored weighting vectors. This approach was successfully used during the lunar-landing phase of Apollo missions.[24]

Several different schemes have been considered for generating the stored weighting vectors. A fairly simple technique which has given excellent performance is essentially as follows: 1) Save the last position and velocity weighting factors computed for each MLS measurement when the filter was operating in a 16-state mode. 2) Scale down the azimuth and elevation angle weighting factors by the current range to the radar divided by the range at the end of the approach phase. 3) Precompute simple weighting factors for processing radar-altimeter data, updating only altitude and vertical velocity.

Simulation results are presented in Table 10 comparing the performance of the stored weighting-vector scheme with that of a 16-state minimum-variance filter at certain key trajectory points. The important point to be seen from Table 10 is that simple stored weighting vectors give essentially the same performance as the 16-state filter. With the 16-state filter the accuracy of the estimate of the range-radar bias error improves as the vehicle approaches the touchdown point. For this reason slightly lower range and altitude errors are obtained. From the viewpoint of touchdown navigation requirements (Table 8), on the other hand, the stored weighting-vector scheme is perfectly acceptable.

Overall System Performance

Typical performance results for the recommended system are presented in Figs. 7 and 8 for the case where TACAN is used as the area navaid, and in Figs. 9-10 for the case where

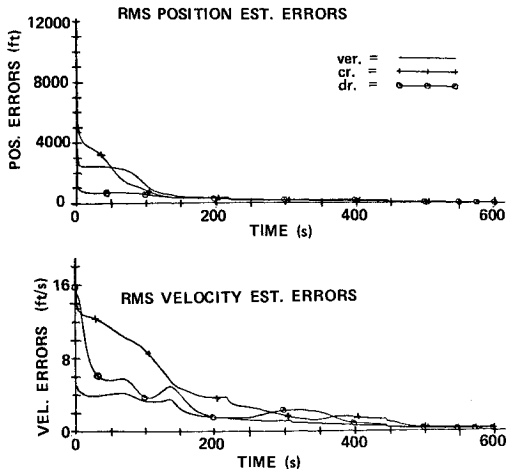

Fig. 7 TACAN/MLS system rms errors.

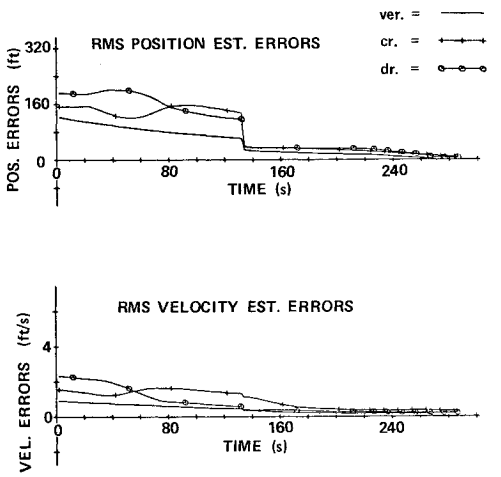

Fig. 8 TACAN/MLS rms errors (last 5 min).

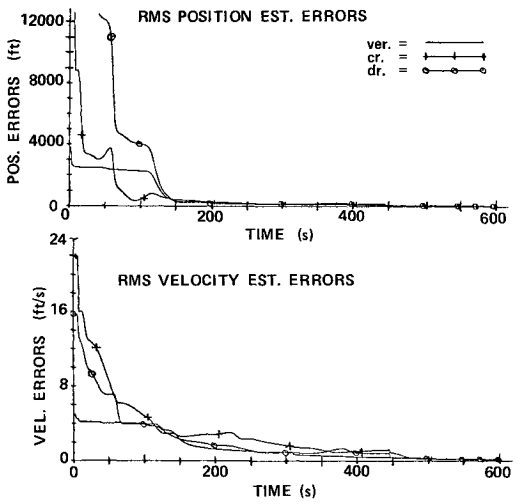

Fig. 9 OWD/MLS system rms errors.

OWD is used. The data are based on linear statistical analysis techniques. A 13-state minimum-variance filter is employed during the approach phase, including IMU alignment-error states. The simple $k_1 \mathbf{b}^T E \mathbf{b}$ scheme is used for underweighting the measurement data. In the terminal phase the stored weighting-vector scheme is employed.

Essentially the same level of performance is obtained with either TACAN or OWD as the area navaid. Position errors are corrected more rapidly when TACAN is used, whereas

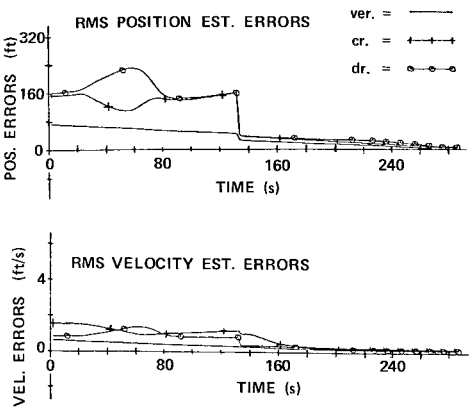

Fig. 10 OWD/MLS rms errors (last 5 min).

velocity errors are corrected more rapidly with OWD. In either case, satisfactory navigation-system performance is obtained.

Conclusions and Recommendations

A 13-state minimum-variance navigation filter is recommended for use during the approach phase (altitude greater than 12,000 ft). Included in the filter as state elements are vehicle position (3), vehicle velocity (3), IMU alignment errors (3), and time-correlated errors (4). All navaid time-correlated errors are modeled as first-order Markov processes. Process noise is included in the state extrapolation process to account for unmodeled errors. A simple underweighting scheme is employed to improve performance during the initial updating period and to insure filter convergence.

For the time-critical terminal phase a 6-state filter is recommended, using only vehicle position and velocity as state elements. The last set of 13-state weighting vectors from the preceding approach phase is saved and used with minor modifications for terminal-phase navigation.

References

[1] Kriegsman, B and Gustafson, D., "Entry Navigation Analysis," *Space Shuttle Integrated Electronics Conference Proceedings,* May 1971, NASA.

[2] Carter, J. P., "Space Shuttle Terminal Navigation with Conventional Navigation Aids," AIAA Paper 72-832, Stanford, Calif., 1972.

[3] Kriegsman, B. and Gustafson, D., "Entry-and-Landing Navigation Study for SSV Orbiter using a PRS Navaid," 23A STS Memo No. 49-71, Oct. 4, 1971, Charles Stark Draper Labs., Cambridge, Mass.

[4] Widnall, W. and Morth, H., "Space Shuttle Landing Navigation Using Precision Distance-Measuring Equipment," Intermetrics Rept. TR13-72 July 1971, Intermetrics, Cambridge, Mass.

[5] Gustafson, D. and Tao, M. "Recent Approach and Landing Navigation Studies," 23A STS Memo. 49-73, May 1973, Charles Stark Draper Labs., Cambridge, Mass.

[6] Kriegsman, B., "Navigation Errors on Various Approach Trajectories," 23A STS Memo No. 41-72, June 1972, Charles Stark Draper Lab., Cambridge, Mass.

[7] McGee, L., et al., "Navigation for Space Shuttle Approach and Landing Using an Inertial Navigation System Augmented by Various Data Sources," *Space Shuttle Integrated Electronics Conf. Proceedings,* May 1971, NASA

[8] Lear, W., "One-way Doppler Derivation, Discussion, and Application to Space Shuttle," Internal Note No. 73-FM-14, Feb. 1973, NASA.

[9] Kriegsman, B. and Gustafson, D., "Drag Measurement as a Possible Means for Reducing Altitude Estimation Errors During SSV Entry," 23A STS Memo No. 10-71, Jan. 1971, Charles Stark Draper Labs., Cambridge, Mass.

[10] Gustafson, D., "A VOR/DME Error Model for SSV Navigation Analysis," MIT STS Memo No. 17-70, June 1970, Charles Stark Draper Labs., Cambridge, Mass.

[11] "Navigation System Characteristics," JSC Internal Note No. 72-FM-190, July 1973, NASA

[12] Lear, W., "Multi-Phase Navigation Program for the Space Shuttle Orbiter," Internal Note No. 73-FM-132, Sept. 1973, NASA.

[13] Broxmeyer, C., *Inertial Navigation Systems,* McGraw Hill, New York, 1964.

[14] Pitman, G., *Inertial Guidance,* Wiley, New York, 1962.

[15] "Theory and Application of Kalman Filtering," AGARD Rept. AG139.

[16] "Special Issue on Linear Quadratic Guidance Problem," *IEEE Transactions on Automatic Control,* Vol. AC-16, Dec. 1971.

[17] Battin, R. H., *Astronautical Guidance,* McGraw-Hill, New York, 1964.

[18] Potter, J. E., "New Statistical Formulas," MIT Instrumentation Lab SGA Memo No. 40, April 1963, Cambridge, Mass.

[19] Kaminski, P., et al., "Discrete Square Root Filtering: A Survey of Current Techniques," *IEEE Transactions on Automatic Control,* Vol. AC-16, Dec. 1971.

[20] Jazwinski, A., *Stochastic Processes and Filtering Theory,* Academic Press, New York, 1970.

[21] Choe, C., "Nonlinear Estimation Theory Applied to the Interplanetary Orbit Determination Problem," *Proceedings of Third Symposium on Nonlinear Estimation Theory and its Applications,* Sept. 1972, pp. 239-245.

[22] Kriegsman, B., et al., "Entry-and-Landing Navigation Filter Studies," Shuttle Memo 10E-74-2, Jan. 1974, Charles Stark Draper Lab., Cambridge, Mass.

[23] Kriegsman, B., "Comparison of Entry-Navigation-Filter Underweighting Schemes with Large Initial-Condition Errors," Shuttle Memo 10E-74-4, Jan. 31, 1974, Charles Stark Draper Lab., Cambridge, Mass.

[24] Kriegsman, B. and Sears, N., "LEM PGNCS and Landing Radar Operations during the Powered Lunar Landing Maneuver," MIT Instrumentation Lab. Rept. E-1982, Aug. 1966, Cambridge, Mass.